BISTATIC COHERENT MIMO CLUTTER RANK ANALYSIS

Kristine Bell,[*] Joel Johnson,[†] Christopher Baker,[†] Graeme Smith,[†] and Muralidhar Rangaswamy[‡]

[*]Metron, Inc., 1818 Library St., Suite 600, Reston, Virginia 20190, USA
[†]Dept. of Electrical and Computer Engineering and ElectroScience Laboratory,
The Ohio State University, Columbus, Ohio, 43210, USA
[‡]U.S. Air Force Research Laboratory, Sensors Directorate, Wright-Patterson AFB, OH, USA

ABSTRACT

The rank of the clutter covariance matrix in a bistatic coherent multiple-input multiple-output (MIMO) radar system with arbitrary planar arrays in both the transmitter and receiver is examined. The analysis provides further generalization of "Brennan's rule" results available for linear arrays in monostatic coherent MIMO and bistatic space-time adaptive processing (STAP) systems. We first extend the two-dimensional (2D) monostatic STAP results of Varadarajan and Krolik (VK) to monostatic MIMO systems with planar arrays. We then use the VK bistatic STAP approach and determine conditions under which a four-dimensional (4D) bistatic MIMO system can be modeled as an equivalent 2D monostatic MIMO system, and apply the 2D results. The analytical expressions are validated against the numerically calculated rank of the theoretical clutter covariance matrix.

Index Terms— MIMO radar, STAP, bistatic, monostatic, clutter rank

1. INTRODUCTION

Monostatic coherent multiple-input multiple output (MIMO) radar for ground moving target indication (GMTI) [1]-[3] is an extension of monostatic single-input multiple output (SIMO) space-time adaptive processing (STAP) [4]-[6], in which multiple transmitter elements emit orthogonal waveforms that are processed separately at each of the receive elements and the scattering responses are coherent across all transmit/receive element pairs. Similarly, bistatic coherent MIMO [7],[8] is a generalization of bistatic STAP [9],[10], in which the transmit and receive elements are located on spatially separated platforms.

In coherent MIMO and STAP systems, the clutter occupies a low-dimensional subspace of the full-dimension data space. The characteristics of the clutter subspace, including its rank, have important implications for the signal processing techniques used to mitigate the clutter as well as overall system performance [1]-[13].

Brennan's rule [4],[11] provides a simple analytical expression for the clutter rank for monostatic STAP when the receive elements are a uniformly spaced linear array (ULA) aligned with the platform velocity vector. In this case the effective spatial sampling is in one dimension (1D) along the array axis, and the scatterer angle-of-arrival (AOA) and Doppler frequency can be expressed in terms of a 1D spatial frequency. In [12], the clutter rank was shown to be determined by the product of the spatial aperture and spatial bandwidth, and Brennan's rule was extended to sub-array geometries. In [2], these 1D results were further extended to the monostatic MIMO case where the transmit array is a linear array aligned with the velocity vector.

In monostatic STAP systems, when the receive array is a planar array or a linear array not aligned with the velocity vector, the effective spatial sampling is in two dimensions (2D) and the scatterer AOA is represented by a 2D spatial frequency. Clutter rank for the 2D monostatic case is analyzed in [10],[13]. In [10], Varadarajan and Krolik (VK) show that the clutter rank is determined by the sum of the aperture-bandwidth products along and orthogonal to the velocity vector. In bistatic STAP systems, the problem expands to one involving a 1D transmit spatial frequency in addition to the 1D or 2D receive spatial frequency and the effective spatial sampling concept does not translate in an obvious manner. In [10], under some some simplifying assumptions, the bistatic STAP problem was converted to an equivalent 2D monostatic STAP problem to which the monostatic results could be applied.

In bistatic MIMO systems with planar arrays, we have 2D spatial frequencies for both the receiver and transmitter. In this paper, we first extend the VK 2D monostatic STAP results to monostatic MIMO systems with planar arrays. We then use the VK bistatic STAP approach and determine conditions under which a four-dimensional (4D) bistatic MIMO system can be modeled as an equivalent 2D monostatic MIMO system, and apply the 2D results. The analytical expressions are validated against the numerically calculated rank of the theoretical clutter covariance matrix for a representative scenario.

This work was supported by the U.S. Air Force Research Laboratory under contract FA9550-14-C-0017. Opinions, interpretations, conclusions, and recommendations are those of the authors and not necessarily endorsed by the U. S. Government.

978-0-9928626-3-3/15/$31.00 ©2015 IEEE

2. BISTATIC COHERENT MIMO MODEL

The bistatic coherent MIMO model presented here is the planar array generalization of the linear array models in [7],[8]. The bistatic coherent MIMO configuration consists of one transmit (TX) platform with M transmit elements and one receive (RX) platform with N receive elements. The transmit and receive arrays are assumed to be planar arrays of omnidirectional elements in general.

We assume the transmit elements emit orthogonal pulsed Doppler waveforms consisting of a sequence of L phase coherent pulses. The signal observed at each receive element is processed by a bank of matched filters for each of the transmitted waveforms. The scattering responses are assumed to be coherent across all of the transmit/receive elements.

The three-dimensional (3D) flat-Earth geometry is shown in Fig. 1. The radar system parameters and various geometrical parameters are defined in Table 1. The coordinate system is defined so that the origin lies directly beneath the receive platform and the baseline between the transmitter and receiver lies along the x-axis. For a given bistatic range R_B, the locus of ground clutter scatterers is an ellipse defined by the equation:

$$\frac{(x-X_c)^2}{a^2}+\frac{y^2}{b^2}=1, \tag{1}$$

where

$$\begin{aligned} X_c &= \frac{X_t}{2}\left[1+\frac{H_r^2-H_t^2}{R_B^2\left(1-e^2\right)}\right] \\ e &= X_t/R_B \\ a &= \frac{R_B}{2}\sqrt{\left[1+\frac{H_r^2-H_t^2}{R_B^2\left(1-e^2\right)}\right]^2-\frac{4H_r^2}{R_B^2\left(1-e^2\right)}} \\ b &= a\sqrt{1-e^2}. \end{aligned} \tag{2}$$

We assume that the returns from the entire clutter ellipse can be approximated as the sum of returns from a large number (N_c) of discrete clutter patches. The ith clutter patch is then modeled as a point scatterer with position $\mathbf{p}_i=[x_i;y_i;0]^T$ and velocity $\dot{\mathbf{p}}_i=\mathbf{0}$. Scatterer parameters are defined in Table 2. These include platform-referenced azimuth and elevation angles, which are shown in Fig. 2 for the receive array.

The measurements from a single clutter patch can be expressed as a vector of the form $\alpha_i\mathbf{v}(\mathbf{p}_i)$, where $\mathbf{v}(\mathbf{p}_i)$ is the $NML\times 1$ MIMO response vector for a scatterer at position $\mathbf{p}_i$ and α_i is the complex clutter return. The α_i are assumed to be zero-mean, uncorrelated random variables with variance P_i, given by the radar equation [8].

The clutter response vector $\mathbf{x}_c$ is then the sum of individual clutter patch returns:

$$\mathbf{x}_c=\sum_{i=1}^{N_c}\alpha_i\mathbf{v}(\mathbf{p}_i), \tag{3}$$

and the clutter covariance matrix is given by:

$$\mathbf{R}_c=E\left\{\mathbf{x}_c\mathbf{x}_c^H\right\}=\sum_{i=1}^{N_c}P_i\mathbf{v}(\mathbf{p}_i)\mathbf{v}(\mathbf{p}_i)^H. \tag{4}$$

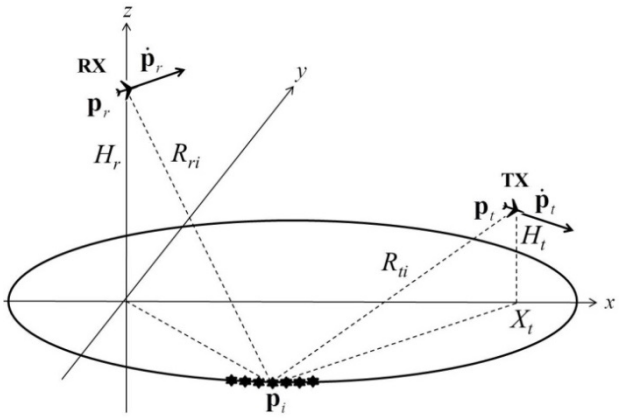

Fig. 1. Bistatic coherent MIMO 3D flat Earth geometry.

Table 1. Bistatic coherent MIMO radar system parameters

Parameter	Definition [units]
L	Number of pulses [-]
M	Number TX elements [-]
N	Number of RX elements [-]
λ	Radar operating wavelength [m]
T_p	Pulse repetition interval [Hz]
$\mathbf{p}_r=[0;0;H_r]^T$	RX platform position [m]
$\dot{\mathbf{p}}_r=v_r\mathbf{i}_{rx}$	RX platform velocity [m/s]
$v_r=\|\dot{\mathbf{p}}_r\|$	RX platform speed [m/s]
δ_r	Angle of RX platform velocity vector wrt system x-axis
$\mathbf{i}_{rx}=\dot{\mathbf{p}}_r/v_r=[\cos\delta_r;\sin\delta_r;0]^T$	RX platform "x"-axis [-]
$\mathbf{i}_{ry}=[-\sin\delta_r;\cos\delta_r;0]^T$	RX platform "y"-axis [-]
$\left(d_{xn}^r,d_{yn}^r\right)$	RX nth element position wrt $\mathbf{i}_{rx},\mathbf{i}_{ry}$ axes [m]
$\mathbf{p}_t=[X_t;0;H_t]^T$	TX platform position [m]
$\dot{\mathbf{p}}_t=v_t\mathbf{i}_{tx}$	TX platform velocity [m/s]
$v_t=\|\dot{\mathbf{p}}_t\|$	TX platform speed [m/s]
δ_t	Angle of TX platform velocity vector wrt system x-axis
$\mathbf{i}_{tx}=\dot{\mathbf{p}}_t/v_t=[\cos\delta_t;\sin\delta_t;0]^T$	TX platform "x"-axis [-]
$\mathbf{i}_{ty}=[-\sin\delta_t;\cos\delta_t;0]^T$	TX platform "y"-axis [-]
$\left(d_{xm}^t,d_{ym}^t\right)$	TX mth element position wrt $\mathbf{i}_{tx},\mathbf{i}_{ty}$ axes [m]

The MIMO response vector has the form:

$$\mathbf{v}(\mathbf{p}_i)=\mathbf{v}_r\left(\mathbf{k}_{ri}(\mathbf{p}_i)\right)\otimes\mathbf{v}_t\left(\mathbf{k}_{ti}(\mathbf{p}_i)\right)\otimes\mathbf{v}_D\left(f_{Di}(\mathbf{p}_i)\right), \tag{5}$$

where $\otimes$ denotes the Kronecker product. The vectors $\mathbf{v}_r\left(\mathbf{k}_{ri}(\mathbf{p}_i)\right)$ and $\mathbf{v}_t\left(\mathbf{k}_{ti}(\mathbf{p}_i)\right)$ are the $N\times 1$ and $M\times 1$ array response vectors of the receive and transmit arrays,

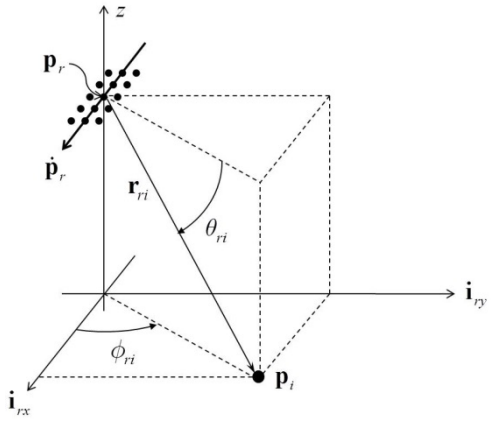

Fig. 2. Receive platform geometry.

Table 2. Scatterer parameters

Parameter	Definition [units]
$\mathbf{p}_i = [x_i; y_i; 0]^T$	Scatterer position [m]
$R_{ri} = \|\mathbf{p}_i - \mathbf{p}_r\|$	RX to scatterer range [m]
$\mathbf{r}_{ri} = (\mathbf{p}_i - \mathbf{p}_r)/R_{ri}$	RX to scatterer unit vector [-]
$R_{ti} = \|\mathbf{p}_i - \mathbf{p}_t\|$	TX to scatterer range [m]
$\mathbf{r}_{ti} = (\mathbf{p}_i - \mathbf{p}_t)/R_{ti}$	TX to scatterer unit vector [-]
$R_B = R_{ti} + R_{ri}$	Bistatic range [m]
$f_{Di} = \frac{1}{\lambda}[\dot{\mathbf{p}}_r^T \mathbf{r}_{ri} + \dot{\mathbf{p}}_t^T \mathbf{r}_{ti}]$	Stationary scatterer Doppler frequency [Hz]
ϕ_{ri}	RX azimuth angle [rad]
θ_{ri}	RX elevation angle [rad]
ϕ_{ti}	TX azimuth angle [rad]
θ_{ti}	TX elevation angle [rad]

respectively. They depend on the scatterer position via the 2D spatial frequency (wavenumber) vectors $\mathbf{k}_{ri}(\mathbf{p}_i) = \left[k_{xi}^r; k_{yi}^r\right]^T$ and $\mathbf{k}_{ti}(\mathbf{p}_i) = \left[k_{xi}^t; k_{yi}^t\right]^T$, whose components are defined as follows:

$$\begin{aligned} k_{xi}^r &= (2\pi/\lambda)\mathbf{i}_{rx}^T \mathbf{r}_{ri} = (2\pi/\lambda)\cos\phi_{ri}\cos\theta_{ri} \\ k_{yi}^r &= (2\pi/\lambda)\mathbf{i}_{ry}^T \mathbf{r}_{ri} = (2\pi/\lambda)\sin\phi_{ri}\cos\theta_{ri} \\ k_{xi}^t &= (2\pi/\lambda)\mathbf{i}_{tx}^T \mathbf{r}_{ti} = (2\pi/\lambda)\cos\phi_{ti}\cos\theta_{ti} \\ k_{yi}^t &= (2\pi/\lambda)\mathbf{i}_{ty}^T \mathbf{r}_{ti} = (2\pi/\lambda)\sin\phi_{ti}\cos\theta_{ti}. \end{aligned} \quad (6)$$

The nth and mth components of the receive and transmit array response vectors, respectively, have the form:

$$\left[\mathbf{v}_r\left(\mathbf{k}_{ri}(\mathbf{p}_i)\right)\right]_n = \exp\left\{j\left[d_{xn}^r k_{xi}^r + d_{yn}^r k_{yi}^r\right]\right\} \quad (7)$$

$$\left[\mathbf{v}_t\left(\mathbf{k}_{ti}(\mathbf{p}_i)\right)\right]_m = \exp\left\{j\left[d_{xm}^t k_{xi}^t + d_{ym}^t k_{yi}^t\right]\right\}, \quad (8)$$

where $\left(d_{xn}^r, d_{yn}^r\right)$ and $\left(d_{xm}^t, d_{ym}^t\right)$ are the positions of the receive and transmit elements, along (x-dimension) and orthogonal to (y-dimension) the platform velocity vectors.

The vector $\mathbf{v}_D\left(f_{Di}(\mathbf{p}_i)\right)$ is the $L\times 1$ Doppler response vector, which depends on the scatterer position via the Doppler frequency, which is given by:

$$f_{Di}(\mathbf{p}_i) = \frac{1}{\lambda}\left[\dot{\mathbf{p}}_r^T \mathbf{r}_{ri} + \dot{\mathbf{p}}_t^T \mathbf{r}_{ti}\right] = \frac{1}{2\pi}\left[v_r k_{xi}^r + v_t k_{xi}^t\right]. \quad (9)$$

The lth component of the Doppler response vector is:

$$\begin{aligned} \left[\mathbf{v}_D\left(f_{Di}(\mathbf{p}_i)\right)\right]_l &= \exp\left\{j2\pi(l-1)T_p f_{Di}(\mathbf{p}_i)\right\} \\ &= \exp\left\{j(l-1)T_p\left[v_r k_{xi}^r + v_t k_{xi}^t\right]\right\}. \end{aligned} \quad (10)$$

If we define

$$d_{xl}^{Dr} \equiv (l-1)T_p v_r; \quad d_{xl}^{Dt} \equiv (l-1)T_p v_t, \quad (11)$$

and use the notation $\{nml\} \equiv ((n-1)M + m - 1)L + l$, then the $\{nml\}$th element of the MIMO response vector can be expressed as:

$$\begin{aligned} \left[\mathbf{v}(\mathbf{p}_i)\right]_{\{nml\}} &= \exp\left\{j\left[\left(d_{xn}^r + d_{xl}^{Dr}\right)k_{xi}^r + d_{yn}^r k_{yi}^r\right]\right\} \\ &\bullet \exp\left\{j\left[\left(d_{xm}^t + d_{xl}^{Dt}\right)k_{xi}^t + d_{ym}^t k_{yi}^t\right]\right\}. \end{aligned} \quad (12)$$

3. CLUTTER RANK ANALYSIS

3.1. Monostatic Case

In the monostatic case, $\mathbf{p}_t = \mathbf{p}_r$ and $\dot{\mathbf{p}}_t = \dot{\mathbf{p}}_r$, therefore the transmit and receive spatial frequencies coincide, i.e. $k_{xi}^t = k_{xi}^r$ and $k_{yi}^t = k_{yi}^r$. Furthermore, the elevation angle $\cos\theta_{ri} = \cos\theta_r$ is constant for all i and the 2D spatial frequency components have the relationship:

$$\left(k_{xi}^r\right)^2 + \left(k_{yi}^r\right)^2 = \left(2\pi/\lambda\right)^2 \cos^2\theta_r, \quad (13)$$

thus the clutter spectrum is a circle in the 2D spatial frequency space, as shown in Fig. 3 (and [10]).

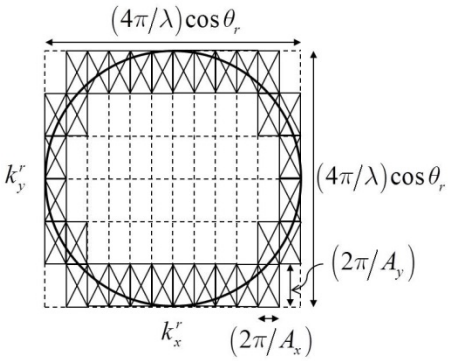

Fig. 3. Monostatic clutter spectrum.

The MIMO response vector in (12) reduces to:

$$\begin{aligned} \left[\mathbf{v}(\mathbf{p}_i)\right]_{\{nml\}} &= \exp\left\{j\left[\left(d_{xn}^r + d_{xm}^t + 2d_{xl}^{Dr}\right)k_{xi}^r\right]\right\} \\ &\bullet \exp\left\{j\left[\left(d_{yn}^r + d_{ym}^t\right)k_{yi}^r\right]\right\}. \end{aligned} \quad (14)$$

This has the form of a spatial array response vector, such as in (7) and (8), with virtual planar array elements at positions $\left(d_{x,nml}^r, d_{y,nml}^r\right) = \left(d_{xn}^r + d_{xm}^t + 2d_{xl}^{Dr}, d_{yn}^r + d_{ym}^t\right)$.

From [10], the effective aperture-bandwidth product is the number of rectangular resolution cells required to "cover" the circular spatial spectrum, where the size of a resolution cell is inversely proportional to the effective aperture of the virtual array, as shown in Fig. 3. The effective aperture in the x and y-dimensions is computed as the maximum difference between any two virtual array

elements in those dimensions plus $\lambda/2$:[1]

$$A_x = \max_{n,m}\left(d^r_{xn}+d^t_{xm}\right)-\min_{n,m}\left(d^r_{xn}+d^t_{xm}\right)+2(L-1)T_p v_r+\frac{\lambda}{2}$$
$$A_y = \max_{n,m}\left(d^r_{yn}+d^t_{ym}\right)-\min_{n,m}\left(d^r_{yn}+d^t_{ym}\right)+\frac{\lambda}{2}. \quad (15)$$

We then find the number of resolution cells in the *x*-and *y*-dimensions as follows:[2]

$$N_x = \left\lceil \frac{(4\pi/\lambda)\cos\theta_r}{(2\pi/A_x)} \right\rceil = \left\lceil A_x \frac{2\cos\theta_r}{\lambda} \right\rceil$$
$$N_y = \left\lceil \frac{(4\pi/\lambda)\cos\theta_r}{(2\pi/A_y)} \right\rceil = \left\lceil A_y \frac{2\cos\theta_r}{\lambda} \right\rceil. \quad (16)$$

If $N_x > 1$ and $N_y > 1$, then the number of cells it takes to cover the spatial spectrum is $2N_x+2N_y-4$, as shown in Fig. 3. We add one to get the clutter rank:

$$\rho_{2D} = 2\left(N_x+N_y\right)-3. \quad (17)$$

The expressions in (15)-(17) provide the MIMO generalization to the 2D STAP results in [10]. The expressions are slightly different than in [10] due to adding the $\lambda/2$ term to the aperture expressions in (15).

If $N_y = 1$, then the spatial spectrum can be covered by N_x resolution cells, and similarly if $N_x = 1$. The problem reduces to the 1D case and the clutter rank is:

$$\rho_{1D} = \begin{cases} N_x+1 & N_y = 1 \\ N_y+1 & N_x = 1. \end{cases} \quad (18)$$

The 1D result for $N_y = 1$ reduces to the Brennan's Rule generalization for MIMO in [2].

3.2. Bistatic Case

In the bistatic case, the spatial frequency relationships are more complicated and the clutter spectrum is a 1D manifold in 4D $\left(k^r_x, k^r_y, k^t_x, k^t_y\right)$ space. From (6), the transmit and receive spatial frequencies satisfy:

$$\left(k^r_{xi}\right)^2+\left(k^r_{yi}\right)^2 = (2\pi/\lambda)^2\cos^2\theta_{ri}, \quad (19)$$

$$\left(k^t_{xi}\right)^2+\left(k^t_{yi}\right)^2 = (2\pi/\lambda)^2\cos^2\theta_{ti}, \quad (20)$$

and the relationship between the transmit and receive spatial frequencies can be written as:

$$k^t_{xi} = c^R_i k^r_{xi} + s^R_i k^r_{yi} - (2\pi/\lambda)c^X_i$$
$$k^t_{yi} = -s^R_i k^r_{xi} + c^R_i k^r_{yi} + (2\pi/\lambda)s^X_i, \quad (21)$$

where

$$c^R_i \equiv (R_{ri}/R_{ti})\cos(\delta_t-\delta_r)$$
$$s^R_i \equiv (R_{ri}/R_{ti})\sin(\delta_t-\delta_r)$$
$$c^X_i \equiv (X_t/R_{ti})\cos\delta_t$$
$$s^X_i \equiv (X_t/R_{ti})\sin\delta_t. \quad (22)$$

Substituting these expressions into (12), we obtain:

$$\left[\mathbf{v}(\mathbf{p}_i)\right]_{\{nml\}} = \exp\left\{ j\left[\left(d^r_{xn}+d^{Dr}_{xl}\right)+\left(d^t_{xm}+d^{Dt}_{xl}\right)c^R_i - d^t_{ym}s^R_i\right]k^r_{xi}\right\}$$
$$\bullet \exp\left\{ j\left[d^r_{yn}+\left(d^t_{xm}+d^{Dt}_{xl}\right)s^R_i + d^t_{ym}c^R_i\right]k^r_{yi}\right\}$$
$$\bullet \exp\left\{ j(2\pi/\lambda)\left[\left(-d^t_{xm}c^X_i + d^t_{ym}s^X_i\right)+d^{Dt}_{xl}c^X_i\right]\right\}. \quad (23)$$

In this paper, we consider situations where the MIMO response vector in (23) has the form of (14) and the bistatic system can be represented by an equivalent 2D monostatic system. This will occur when the argument in the third line of (23) is equal to zero, which requires one of the following conditions to be satisfied:

i. $X_t \ll R_{ti}$ and therefore $c^X_i \approx 0$ and $s^X_i \approx 0$. This is similar to the "quasi-monostatic" assumption in [10].
ii. $\delta_t = 90^\circ$ ($c^X_i = 0$) and $d^t_{ym} = 0 \ \forall m$, i.e. the transmit platform velocity is perpendicular to the baseline between the transmitter and receiver, and the transmit array is a linear array aligned with the velocity vector.
iii. $v_t = 0$ ($d^{Dt}_{xl} = 0 \ \forall l$) and $\left(d^t_{xm}, d^t_{ym}\right) = d_m\left(\sin\delta_t, \cos\delta_t\right)$, i.e. the transmitter is stationary and the transmit array is a linear array aligned perpendicular to the baseline between the transmitter and receiver, regardless of the arbitrarily defined (when $v_t = 0$) angle δ_t.

The MIMO response vector then has the form of (14) with virtual planar array elements at positions given by the terms in the square brackets in the first two terms in (23). Unfortunately, these virtual element positions vary with clutter patch index through the terms c^R_i and s^R_i, which depend on the ratio R_{ri}/R_{ti}. For simplicity, we use the average ratio, which we assume is approximately equal to one, $\left(R_{ri}/R_{ti}\right)_{av} \approx 1$, and define:

$$c^{tr} \equiv \cos(\delta_t-\delta_r); \quad s^{tr} \equiv \sin(\delta_t-\delta_r). \quad (24)$$

The virtual array elements then become:

$$d^r_{x,nml} \approx \left(d^r_{xn}+d^{Dr}_{xl}\right)+\left(d^t_{xm}+d^{Dt}_{xl}\right)c^{tr} - d^t_{ym}s^{tr}$$
$$d^r_{y,nml} \approx \left[d^r_{yn}+\left(d^t_{xm}+d^{Dt}_{xl}\right)s^{tr}+d^t_{ym}c^{tr}\right], \quad (25)$$

and the effective apertures are found from:

$$A_x = \max_{n,m,l}\left(d^r_{x,nml}\right)-\min_{n,m,l}\left(d^r_{x,nml}\right)+\frac{\lambda}{2}$$
$$A_y = \max_{n,m,l}\left(d^r_{y,nml}\right)-\min_{n,m,l}\left(d^r_{y,nml}\right)+\frac{\lambda}{2}. \quad (26)$$

The 2D clutter spectrum defined in (19) is no longer a circle centered at the origin, however it is an oval-shaped region, as shown in Fig. 4 for the example in Section 4.

To find N_x and N_y, we first determine the spectral extent in the *x*- and *y*-dimensions from the maximum and minimum values of k^r_{xi} and k^r_{yi} in (19), and then N_x and N_y are given by:

$$N_x = \left\lceil \frac{\left(k^r_{xi}\right)_{\max}-\left(k^r_{xi}\right)_{\min}}{(2\pi/A_x)} \right\rceil = \left\lceil A_x \frac{\left(k^r_{xi}\right)_{\max}-\left(k^r_{xi}\right)_{\min}}{2\pi} \right\rceil$$
$$N_y = \left\lceil \frac{\left(k^r_{yi}\right)_{\max}-\left(k^r_{yi}\right)_{\min}}{(2\pi/A_y)} \right\rceil = \left\lceil A_y \frac{\left(k^r_{yi}\right)_{\max}-\left(k^r_{yi}\right)_{\min}}{2\pi} \right\rceil. \quad (27)$$

The clutter rank can then be found from (17) or (18).

The expressions in (24)-(27) and (17) provide the

[1] Each discrete element provides an effective continuous aperture of length $\lambda/2$, the spatial Nyquist sampling interval [14].
[2] The notation $\lceil \bullet \rceil$ denotes rounding up to an integer.

MIMO generalization to the 2D bistatic STAP results in [10]. The expressions are slightly different than in [10] due to adding the $\lambda/2$ term to the aperture expressions in (26), approximating the range ratio as one in (25), and in the method for computing the spectral extent in (27).

4. EXAMPLE

We consider the following scenario: $N = 10$, $M = 5$, $L = 16$, $\lambda = 1.33$ m, $T_p = 1/300$ s, $H_r = 2$ km, $v_r = 100$ m/s, $\delta_r = 0°$, $X_t = 5$ km, $H_t = 1$ km, $v_t = 75$ m/s, $\delta_t = 90°$. The RX array is a ULA with $\lambda/2$ spacing rotated 3° with respect to the receive velocity vector. The TX array is a ULA with $\lambda/2$ spacing aligned with the transmit velocity vector. We consider bistatic ranges from 7 km to 25 km.

The receive clutter spectra are shown in Fig. 4. At 25 km, the spectrum looks similar to the monostatic case, but as the range decreases, the bistatic geometry causes the spectra to become smaller, more oval-shaped, and shifted up and to the left of the origin.

The normalized eigenvalues of the clutter covariance matrix and the predicted rank are shown in Fig. 5. The eigenvalues do not show a sharp drop-off thus it is hard to say what the "correct" rank is. The predicted ranks are all at the 99.9th percentile (or greater) of total energy. The clutter rank is significantly less than $NML = 800$, and decreases as bistatic range decreases due to the smaller extent of the spatial spectrum observed in Fig. 4.

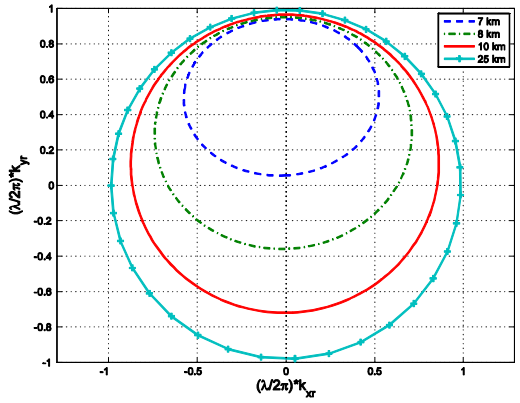

Fig. 4. Bistatic clutter spectrum for bistatic ranges varying from 7 km to 25 km.

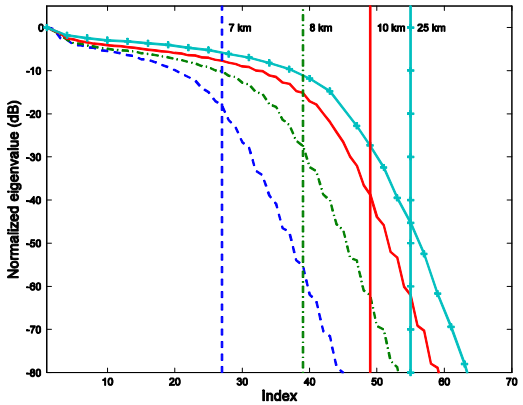

Fig. 5. Normalized eigenvalues and predicted clutter rank (vertical lines) for bistatic ranges varying from 7 km to 25 km.

5. SUMMARY

In this paper, we analyzed the rank of the clutter covariance matrix in a bistatic coherent MIMO radar system with arbitrary planar arrays in both the transmitter and receiver. We first extended the VK 2D monostatic STAP results to monostatic MIMO systems with planar arrays, then determined conditions under which a 4D bistatic MIMO system could be modeled as an equivalent 2D monostatic MIMO system, and applied the 2D results. The analytical expressions were validated against the numerically calculated rank of the theoretical clutter covariance matrix for a representative scenario.

REFERENCES

[1] J. Li and P. Stoica, "MIMO Radar with Colocated Antennas," *IEEE Signal Process. Mag.*, vol. 24, no. 9, pp. 106-114, Sep. 2007.

[2] C.-Y. Chen and P. P. Vaidyanathan, "MIMO Radar Space-Time Adaptive Processing Using Prolate Spheroidal Wave Functions," *IEEE Trans. Signal Process.*, vol. 56, no. 2, pp. 623-635, Feb. 2008.

[3] J. M. Kantor and D. W. Bliss, "Clutter Covariance Matrices for GMTI MIMO radar," in *Proc. 44th Asilomar Conf. Signals, Syst., Comput.*, Pacific Grove, CA, pp. 1821-1826, Nov. 2010.

[4] J. Ward, "Space-Time Adaptive Processing for Airborne Radar," MIT Lincoln Laboratory Tech. Report 1015, DTIC No. ESC-TR-94-109, Dec. 1994.

[5] J. R. Guerci, *Space-Time Adaptive Processing for Radar*, Norwood, MA: Artech House, 2003.

[6] R. Klemm, *Principles of Space-Time Adaptive Processing, 3rd ed.*, London, UK: The Institution of Engineering and Technology, 2006.

[7] J. Li, G. Liao, and H. Griffiths, "Bistatic MIMO Radar Space-Time Adaptive Processing," in *Proc. IEEE Radar Conf.*, Kansas City, MO, pp. 498-502, May 2011.

[8] K. L. Bell, J. T. Johnson, C. J. Baker, G. E. Smith, and M. Rangaswamy, "Modeling and Simulation for Multistatic Coherent MIMO Radar," in *Proc. IEEE Radar Conf.*, Ottawa, CN, Apr. 2013.

[9] Y. Zhang and B. Himed, "Bistatic Space-Time Adaptive Processing (STAP) for Airborne/Spaceborne Applications," AFRL Tech. Report AFRL-SN-RS-TR-1999-97, May 1999.

[10] V. Varadarajan and J. L. Krolik, "Joint Space-Time Interpolation for Distorted Linear and Bistatic Array Geometries," *IEEE Trans. Signal Process.*, vol. 54, no. 3, pp. 848-860, Mar. 2006.

[11] L. E. Brennan and F. M. Staudaher, "Subclutter Visibility Demonstration," Adaptive Sensors, Inc., Santa Monica, CA Tech. Report RL-TR-92-21, 1992.

[12] Q. Zhang and W. B. Mikhael, "Estimation of the Clutter Rank in the Case of Subarraying for Space-Time Adaptive Processing," *Electronics Letters*, vol. 33, no. 5, pp. 419-420, 27 Feb. 1997.

[13] N. A. Goodman and J. M. Stiles, "On Clutter Rank Observed by Arbitrary Arrays," *IEEE Trans. Signal Process.*, vol. 55, no. 1, pp. 178-186, Jan. 2007.

[14] H. L. Van Trees, *Optimum Array Processing*, New York, NY: Wiley, 2002.